



## Carbon Nanotubes Flow on Mixed Convection of Aligned Magnetohydrodynamics over a Static/Moving Wedge with Convective Boundary Conditions

Siti Shuhada Ishak<sup>1</sup>, Nurin Nisa Mohd Noor Azhar<sup>1</sup>, Nurul Syafiqah Nazli<sup>1</sup>, Mohd Rijal Ilias<sup>1</sup>, Roselah Osman<sup>1</sup>, Zubaidah Sadikin<sup>1,\*</sup>, Abdul Rahman Mohd Kasim<sup>2</sup>, Nurul Farahain Mohammad<sup>3</sup>

<sup>1</sup> School of Mathematical Sciences, College of Computing, Informatics and Media, Universiti Teknologi MARA, 40450 Shah Alam, Selangor, Malaysia

<sup>2</sup> Centre for Mathematical Sciences, College of Computing & Applied Sciences, Universiti Malaysia Pahang, Lebuhraya Tun Razak, Gambang 26300, Pahang, Malaysia

<sup>3</sup> Department of Computational and Theoretical Sciences, Kulliyah of Science, International Islamic University Malaysia, Bandar Indera Mahkota, 25200 Kuantan, Pahang, Malaysia

### ARTICLE INFO

#### Article history:

Received 11 August 2022

Received in revised form 13 September 2022

Accepted 10 October 2022

Available online 1 July 2023

#### Keywords:

Aligned MHD; Mixed Convection; Convective Boundary Condition; Moving Wedge; Carbon Nanotubes

### ABSTRACT

Nanotubes have been designed to be significantly larger than any other material, and these cylindrical carbon molecules have exceptional properties that are important for nanoscience and nanotechnology. Due to their exceptional thermal conductivity and mechanical and electrical properties, carbon nanotubes are used as additives to improve heat transfer in various industrial applications. The study analyzed a steady, two-dimensional, carbon nanotubes (CNTs) flow on aligned magnetohydrodynamics mixed convection over a static or moving wedge with convective boundary conditions. The CNTs used are single-wall carbon nanotubes (SWCNTs), multi-wall carbon nanotubes (MWCNTs), and water as the base fluid. The similarity transformation was used to reduce the partial differential governing equations into ordinary differential equations. Then, the reduced equations were solved using fourth-fifth order Runge–Kutta–Fehlberg and coded into Maple Software. The results of velocity and temperature profiles were illustrated graphically while the results of skin friction coefficient and Nusselt number were presented in tabulated data. It is found that the velocity profiles increase, and temperature profiles decrease when the angle of aligned magnetic field parameter, the interaction of magnetic parameter, convective parameter, and total angle of the wedge parameter number increase. For case where Biot number and volume fraction of nanoparticles parameters increase, the velocity profiles decrease, and temperature profiles increase. SWCNTs have increased skin friction and Nusselt numbers due to their higher density and thermal conductivity compared to MWCNTs. The finding of this study will benefit the who works in research and development in a range of industries and the mathematics body of knowledge as it provides new information to people who are interested in this field.

\* Corresponding author.

E-mail address: [zubaidah1590@uitm.edu.my](mailto:zubaidah1590@uitm.edu.my) (Zubaidah Sadikin)

<https://doi.org/10.37934/cfdl.15.7.7491>

## 1. Introduction

In the field of industrial and technological applications, nanofluids play an important role due to their superior physical, chemical and thermal performance. The purpose of using nanofluids is to increase the thermal conductivity of the fluid. One of the techniques, to increase the effective thermal conductivity of this mass transfer fluid, is to add nanoparticles or nanotubes in the base fluid. Choi [1] was the first to study heat transfer in nanofluids. According to Choi [1] and Eastman *et al.*, [2], a nanofluid is a fluid composed of nanoparticles dispersed in a base fluid. Khan *et al.*, [3] noted that a variety of nanoparticles are commonly used in nanofluids, including copper (Cu), iron (Fe), CNTs, and others. CNTs are allotropes of carbon with a cylindrical nanostructure and are used in a wide variety of fields, including optics, microelectronics cooling, nanotechnology, chemical production, and many other areas of material science [4-6]. There are two types of CNTs: single-wall carbon nanotubes (SWCNTs) and multiwall carbon nanotubes (MWCNTs) [7, 8]. SWCNTs are monolayers, while MWCNTs consist of multiple layers of graphene. The effects of SWCNTs and MWCNTs were evaluated over a static or moving wedge with convective boundary condition with aligned MHD presence for this study.

Fluid boundary layer flow plays a significant role in spreading knowledge given the growing interest in the theory in a wide range of physical problems. The boundary layer flow over wedges has recently become a popular subject in fluid mechanics due to its many applications in thermal engineering, such as heat exchangers, heat insulators, geothermal systems, crude oil extraction, and nuclear waste storage. A steady laminar flow past a fixed wedge was first analysed by Falkner and Skan [9] to illustrate Prandtl's boundary layer theory. This equation a form  $ax^m$ , where  $x$  is the coordinate measured along the wedge wall and  $a$  ( $>0$ ), and  $m$  are constants and its similar solution was later studied by Hartree [10] and Koh and Hartnett [11]. The investigations on nanofluids over a wedge were made by a lot of researchers and they obtained lots of valuable results. Ilias *et al.*, [12-14] studied the nanofluids flow past a static wedge using the Keller-box method. They found that the magnetic parameter significantly influences fluid velocity, temperature, skin friction, and heat transfer rates for both steady and unsteady flow. Pandey and Kumar [15] investigated a nanofluids flow over a wedge with the thermal radiation, viscous dissipation, and chemical reactions effects. They found that an increase in solid volume fraction of nanofluids with the magnetic parameter, the skin friction coefficient decreases, and for Nusselt number and Sherwood number shown the opposite behaviours. The permeable moving and stationary wedge are studied by Ishak *et al.*, [16]. They found that the velocity profiles and Nusselt numbers of moving wedges are higher, but the temperature profiles and skin friction are lower than those of stationary and moving against flow wedges. Kandasamy *et al.*, [17] investigated the SWCNTs in the presence of water and seawater with variable stream conditions over a porous wedge with the effect of solar radiation energy. They found that the thermal boundary layer of SWCNTs-water absorbs incident solar radiation and transmits it to the working fluid convection, compared to Cu-water. Berrehal *et al.*, [18] studied MWCNTs with water as the base fluid flowing over a wedge with thermal radiation and found that heat transfer irreversibility becomes dominant near the surface of the wedge when the radiation parameter decreases, in contrast to the behaviour of the nanoparticles volume fraction.

Several studies have been conducted on the heat transfer enhancement of nanofluids flowing through CNTs under magnetohydrodynamics (MHD) effects over a wedge. Amar [19] studied the impact of the viscous dissipation, thermophoresis, Brownian motion on MHD fluid boundary layer flow past a wedge with heat and mass transfer of nanofluids. Based on the study, an increase the magnetic field effect shows an increase in local Sherwood number and skin-friction but decrease in Nusselt number and concentration profile. Venkataramanaiah *et al.*, [20] studied MHD flow and heat

transfer from water-functionalized CNTs over a static or moving wedge. They found that the magnetic field reduces boundary layer thickness and increases skin friction and Nusselt numbers. SWCNTs also offer higher skin friction and Nusselt numbers due to their higher density and thermal conductivity. In the presence of a heat source or sink, it was found that a magnetic field increases skin friction and heat transfer rates. The MHD flow and heat transfer from water functionalized CNTs over a static/moving wedge are studied by Khan *et al.*, [21]. It is shown that the magnetic field reduces boundary layer thickness and increases skin friction and Nusselt numbers. Due to higher density and thermal conductivity, SWCNTs offer higher skin friction and Nusselt numbers. Noranuar *et al.*, [22, 23] studied a mixture of water-based single-wall and multi-wall CNTs with the effect of MHD. They found that the CNTs' magnetic field decreases both the temperature and velocity of the CNT nanofluids. However, when human Casson blood is used as nanoparticles, the results found that the temperature and velocity profiles increase with the incorporation of CNTs. Alqahtani *et al.*, [24] studied sodium alginate-based carbon nanotubes with MHD stagnation-point flow on a convective heated stretching disk with viscous dissipation and suction effects. They found that the magnetic field increases velocity and skin friction. Based on this theoretical literature [19-24], the influence of MHD makes an increasingly important contribution to thermal conductivity in CNTs. The studies on the magnetic field effect were discovered by another researcher [25-27] was discuss in different situation.

In general, convection is a heat transfer mechanism involving the movement of fluid from a hotter to a colder medium. Mixed convection flow and heat transfer within various geometries flow has many engineering applications. The investigation of mixed convection flow in various types of fluid are increasingly interested by the researchers. The behaviour of boundary layers in forced flow over a wedge was investigated by Watanabe [28]; Khan, Culham, & Haq [21]; Yih [29] and Mahood, Shafiq, Khan, & Badruddin [30]. The result for various values of pressure gradient parameter ( $m$ ) have a substantial influence on fluid velocity. Mishra *et al.*, [31] also looked at the flow of mixed convection nanofluids across a wedge with a magnetic field presence. When it comes to velocity, the magnetic field is more effective. Waini *et al.*, [32] discovered that as the mixed convection parameter is reduced, the velocity distribution decelerates in their study. The studies on the mixed convection were discovered by the researcher [33, 34] was discuss in different situation.

Convective boundary conditions also play a crucial role in many engineering processes and industries. Anuar *et al.*, [35] study a convective boundary condition over a moving wedge in nanofluid. They found that a larger value in convective parameter show an increasing behaviour for temperature and local Nusselt number. Hussain *et al.*, [36] discussed on the fluid over a penetrable stretching wedge in the existence of nonlinear radiation and convective boundary condition. They found that an increased value of convective parameter shows an increases Nusselt number and decreases skin friction coefficient. Another study in convective boundary condition with the different geometries' situation such as Ilias *et al.*, [37] who study the influence of aligned and transverse magnetic field on two-dimensional natural convection boundary layer flow in the presence of convective boundary condition. Bosli *et al.*, [38] investigation of aligned MHD nanofluid with convective boundary condition. Rosaidi *et al.*, [39] investigate the behaviour of MHD free convection flow of magnetic nanofluids over a moving vertical plate with convective boundary conditions. Based on their study, an increase the convective parameter shows that increase the heat transfer and skin fraction.

Based on these previous studies, this study investigates the aligned MHD mixed convection water-functionalized carbon nanotubes flow over a static or moving wedge with convective boundary conditions. The solutions are solved using the fourth-fifth order Runge-Kutta-Fehlberg method and displayed and analysed graphically.

## 2. Mathematics Formulation

This study considers steady two-dimensional boundary layer flow past a static or a moving wedge in a water-based nanofluids containing SWCNTs and MWCNTs. The nanofluids is assumed incompressible and the flow is assumed to be steady and laminar. It is also assumed that the base fluid (i.e., water) and the nanoparticles are in thermal equilibrium and no slip occurs between them.

A Cartesian coordinate system  $(x, y)$ , where  $x$  and  $y$  are the coordinates measured along the surface of the wedge and normal to it, respectively as shown in Figure 1. The wedge surface is retained by convective heat transfer  $T_f$ . Meanwhile the temperature  $T_\infty$  is the ambient fluid temperature. The magnetic strength  $B(x)$  is applied to the flow with acute angle  $\alpha$  along  $y$  direction. It is assumed that wedge is moving with the velocity  $U_w(x) = U_w x^m$  and the free stream velocity  $U_e(x) = U_\infty x^m$  where  $U_w$  and  $U_\infty$  are constants. The wedge's total angles are  $\Omega = \lambda\pi$ , where  $\lambda = \frac{2m}{1+m}$  which refers to angle parameter and  $m$  is the pressure gradient parameter. It is also assumed that the induced magnetic field caused by the motion of electrically conducting fluid is neglected, as it is very small compared to magnetic field. Considering the known modelling of Tiwari and Das [7], under the boundary layer approximations, the basic steady conservation of mass, momentum, and energy equations can be written as based on [9-14]:

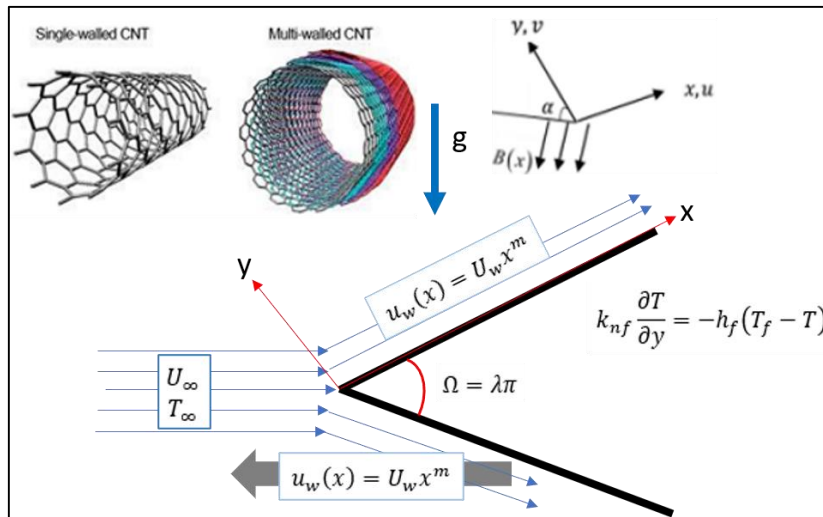


Fig. 1. The schematic diagram of the problem and coordinate system

$$\frac{\partial u}{\partial x} + \frac{\partial v}{\partial y} = 0 \quad (1)$$

$$u \frac{\partial u}{\partial x} + v \frac{\partial u}{\partial y} = U_e \frac{\partial U_e}{\partial x} + \frac{\mu_{nf}}{\rho_{nf}} \frac{\partial^2 u}{\partial y^2} - \frac{\sigma B^2(x)}{\rho_{nf}} \sin^2 \alpha (u - U_e) + \frac{(\rho\beta)_{nf}}{\rho_{nf}} g (T - T_\infty) \sin \frac{\Omega}{2} \quad (2)$$

$$u \frac{\partial T}{\partial x} + v \frac{\partial T}{\partial y} = \alpha_{nf} \frac{\partial^2 T}{\partial y^2} \quad (3)$$

The boundary conditions for the velocity and temperature of this problem are given by:

$$u = U_w(x), \quad v = 0, \quad k_{nf} \frac{\partial T}{\partial y} = -h_f (T_f - T), \quad \text{on } y = 0 \quad (4)$$

$$u = U_e(x), \quad T = T_\infty \quad \text{as } y \rightarrow \infty$$

where  $u$  and  $v$  denote the velocity components in  $x$ - and  $y$ -directions respectively,  $\nu$  is kinematic viscosity,  $\sigma$  is the electrical conductivity,  $B(x) = B_0 x^{\frac{m-1}{2}}$  is magnetic field with  $B_0$  the strength of the magnetic field,  $T$  is the temperature of the fluid,  $T_f$  is the hot fluid at uniform temperature,  $T_\infty$  is the constant temperature of ambient cold fluid,  $g$  is the gravity acceleration and  $h_f$  is the heat transfer coefficient of fluid in term of  $h_f = c\sqrt{(m+1)x^{m-1}}$  is the convective heat transfer coefficient arises from convective boundary conditions where  $c$  is a constant. The effective properties of magnetic nanofluids for CNTs may be expressed in terms of the properties of base fluids, nanoparticles, and the volume fraction of solid nanoparticles as follow [8, 21]:

$$\rho_{nf} = (1 - \phi)\rho_f + \phi\rho_{CNT}, \quad \mu_{nf} = \frac{\mu_f}{(1 - \phi)^{2.5}},$$

$$(\rho C_p)_{nf} = (1 - \phi)(\rho C_p)_f + \phi(\rho C_p)_{CNT}, \quad (\rho\beta)_{nf} = (1 - \phi)(\rho\beta)_f + \phi(\rho\beta)_{CNT} \quad (5)$$

$$\alpha_{nf} = \frac{k_{nf}}{(\rho C_p)_{nf}}, \quad \beta_{nf} = (1 - \phi)\beta_f + \phi\beta_{CNT},$$

$$\frac{k_{nf}}{k_f} = \left(1 - \phi + 2\phi \frac{k_{CNT}}{k_{CNT} - k_f} \ln \frac{k_{CNT} + k_f}{2k_f}\right) \times \left(1 - \phi + 2\phi \frac{k_f}{k_{CNT} - k_f} \ln \frac{k_{CNT} + k_f}{2k_f}\right)^{-1}$$

where  $\phi$  is the volume fraction of nanoparticle,  $\mu_{nf}$  is the effective dynamic viscosity,  $\rho_{nf}$  is the effective density,  $(\rho\beta)_{nf}$  is the thermal expansion coefficient,  $\alpha_{nf}$  is the thermal diffusivity of the fluid,  $k_{nf}$  is the thermal conductivity of the nanofluids,  $\rho_f$  is the effective density of fluid,  $(\rho C_p)_{nf}$  is the heat capacity of CNTs,  $\mu_f$  is the effective dynamic viscosity of fluid,  $k_f$  is the thermal conductivity of the fluid,  $k_{CNT}$  is the thermal conductivity of CNTs and  $(\rho\beta)_{CNT}$  is the thermal expansion coefficient of CNTs.

The continuity (1) is satisfied by introducing a stream function  $\psi(x, y)$  such as:

$$u = \frac{\partial \psi}{\partial y}, \quad v = -\frac{\partial \psi}{\partial x} \quad (6)$$

The following similarity variables are introduced to solve the governing equations in Eq. (1) to Eq. (3), as in the study by [12-14]:

$$\eta = \left[\frac{m+1}{2x^2} Re_x\right]^{\frac{1}{2}} y, \quad \psi = \left[\frac{2\nu_f^2 Re_x}{m+1}\right]^{\frac{1}{2}} f(\eta), \quad \theta = \frac{T - T_\infty}{T_f - T_\infty} \quad (7)$$

where  $\eta$  is the similarity variable,  $Re_x = \frac{U_e x}{\nu_f}$  is the Reynolds number,  $U_e = U_\infty x^m$  and  $f(\eta)$  the non-dimensional stream function and  $\theta(\eta)$  the non-dimensional temperature.

By substitute Eq. (5), Eq. (6) and Eq. (7) into Eq. (2) and Eq. (3), the following nonlinear systems of ordinary differential equations were obtained

$$\begin{aligned}
 & f'''(\eta) + \left[ (1 - \phi)^{2.5} \left( 1 - \phi + \phi \left( \frac{\rho_{CNT}}{\rho_f} \right) \right) \right] \left[ f(\eta)f''(\eta) + \lambda \left( 1 - (f'(\eta))^2 \right) \right] \\
 & - (2 - \lambda)(1 - \phi)^{2.5} M \sin^2 \alpha (f'(\eta) - 1) \\
 & + (2 - \lambda) \left[ 1 - \phi + \phi \left( \frac{(\rho\beta)_{CNT}}{(\rho\beta)_f} \right) \right] (1 - \phi)^{2.5} \lambda_T \sin \frac{\Omega}{2} = 0
 \end{aligned} \tag{8}$$

$$\frac{\frac{k_{nf}}{k_f}}{\left( 1 - \phi + \phi \frac{(\rho C_p)_{CNT}}{(\rho C_p)_f} \right)} \frac{1}{Pr} \theta''(\eta) - f(\eta)\theta'(\eta) = 0 \tag{9}$$

Subjected to the boundary conditions (4), which becomes:

$$\begin{aligned}
 & f(0) = 0, \quad f'(0) = \varepsilon, \quad \theta'(0) = -Bi(1 - \theta(0)) \quad \text{on } \eta = 0 \\
 & f'(\eta) = 1, \quad \theta(\eta) = 0, \quad \text{as } \eta \rightarrow \infty
 \end{aligned} \tag{10}$$

where primes denote differentiation with respect to  $\eta$ ,  $M$  is the magnetic parameters where  $M = \sigma B_0^2 / \rho U_\infty$ ,  $Gr = g\beta_f(T_w - T_\infty)x^3 / \nu_f^2$  is the Grashof number,  $\lambda_T = \frac{Gr_x}{Re^2}$  is the buoyancy parameter or mixed convection parameter,  $\Omega = \lambda\pi$  is the total angle of wedge, where  $\lambda = \frac{2m}{m+1}$  which refers to angle parameter and  $m$  is the pressure gradient parameter,  $Pr$  is the Prandtl number,  $Pr = (\mu C_p)_f / k_f$  and Biot number is the  $Bi = \frac{c}{k_{nf}} \sqrt{\left( \frac{2\nu_f}{U_\infty} \right)}$ . Note that  $\varepsilon$  denotes the direction of motion of the plate. Here  $\varepsilon = 0$  for the static wedge, while  $\varepsilon < 0$  is for the wedge and the fluid move in the opposite direction and  $\varepsilon > 0$  indicates the wedge and the fluid move in the same. The quantities of engineering interest are the local skin friction coefficient,  $C_f$  at the surface of the plate and local Nusselt number,  $Nu_x$  which are defined as:

$$C_f = \frac{\tau_w}{\rho_f U_\infty^2}, \quad Nu_x = \frac{xq_w}{k_f(T_f - T_\infty)} \tag{11}$$

where  $\tau_w$  is the wall skin friction or shear stress at the plate and  $q_w$  is the heat flux from the plate, which given by:

$$\tau_w = \mu_{nf} \left( \frac{\partial u}{\partial y} \right)_{y=0}, \quad q_w = -k_{nf} \left( \frac{\partial T}{\partial y} \right)_{y=0} \tag{12}$$

Substituting Eq. (5) – Eq. (7) into Eq. (12) and using Eq. (11), the non-dimensional skin friction coefficient and local Nusselt number written as:

$$C_f(Re_x)^{\frac{1}{2}} = \sqrt{\frac{m+1}{2}} \frac{f''(0)}{(1-\phi)^{2.5}},$$

$$\frac{Nu_x}{(Re_x)^{\frac{1}{2}}} = -\sqrt{\frac{m+1}{2}} \frac{k_{nf}}{k_f} \theta'(0)$$
(13)

### 3. Method of Solution

In order to solve the nonlinear system of differential Eq. (8) and Eq. (9) with the boundary conditions Eq. (10), the Runge-Kutta-Fehlberg fourth-fifth method by using a software Maple 20. The system of non-linear ordinary differential with boundary conditions will be solved numerically utilizing Maple dsolve command with option numeric. This software automatically detected fourth and fifth order Runge–Kutta–Fehlberg method to solve the two-point boundary value problem. The RKF45 uses both fourth and fifth order Runge–Kutta scheme.

The results of the current study were compared to the results of a previous study to validate the validity and correctness of the present analysis, the numerical values of skin friction coefficient are derived and compared with four studies which are Watanabe [28], Khan, Culham, & Haq [21], Yih [29] and Mahood, Shafiq, Khan, & Badruddin [30], as shown in Table 1 below. The reported results are in good agreement with the previous researchers.

**Table 1**  
 Comparison Result of  $f'(0)$  for Different Values of  $m$  when  $\alpha = M = \lambda_T = \phi = Bi = 0$

$m$	(Iterative numerical quadratures method) [28]	(Quasi linearization technique) [21]	(keller Box method) [29]	(Runge-Kutta Fehlberg with shooting technique) [30]	Present result (RK45F)
0.0	0.46960	0.4696	0.469600	0.469599988	0.469604
0.0141	0.50461	-	0.504614	0.504614318	0.504618
0.0435	0.58698	-	0.568978	0.568977764	0.568982
0.0909	0.65498	0.6550	0.654974	0.654993688	0.654983
0.1429	0.73200	-	0.73200	0.731998540	0.732003
0.2	0.80213	0.8021	0.802125	0.802125593	0.802131
0.3333	0.92765	0.9277	0.927653	0.927653591	0.927660
0.5	-	1.0389	-	1.038903483	1.038911
1	-	1.2326	1.232588	1.232587657	1.232598

### 4. Results

The results of different variations of flow parameters are presented and discussed as above. The thermophysical properties of the CNTs and base fluid are given in Table 2. The parameters used for simulation are  $\alpha = 45^\circ$ ,  $M = 2$ ,  $\lambda = 0.3333$ ,  $\lambda_T = 0.3$ ,  $\phi = 0.1$  and  $Bi = 0.1$ , unless otherwise stated:

**Table 2**  
 Thermophysical Properties of Carbon Nanotube and Base Fluid  
 [21, 40, 41]

Physical Properties	SWCNT	MWCNT	Base Fluid (water)
$\rho(kg/m^3)$	2600	3000	997.1
$C_p(J/kgK)$	425	796	4179
$k(W/mK)$	6600	1600	0.613
$\beta \times 10^{-5}(K^{-1})$	2.6	2.8	21
Pr			6.2

Figure 2 to Figure 7 shows how velocity and temperature profiles change with different values  $\alpha$ ,  $\lambda$ ,  $M$ ,  $\lambda_T$ ,  $\phi$  and  $Bi$ . While the numerical value of skin friction coefficient and Nusselt number for SWCNTs-water and MWCNTs-water are shown in Table 3 and Table 4.

Figure 2(a) and Figure 2(b) shows the effect of inclination angle of magnetic field,  $\alpha$  on velocity and temperature profiles of SWCNTs and MWCNTs for  $\varepsilon = -0.2$ ,  $\varepsilon = 0$  and  $\varepsilon = 0.2$ . It is observed for every type of CNTs and all conditions of the wedges that with an increase in  $\alpha$ , while the other parameters which are  $\lambda = 0.3333$ ,  $M = 2$ ,  $\lambda_T = 0.3$ ,  $\phi = 0.1$  and  $Bi = 0.1$  are kept constant. It shows that for all three cases of  $\varepsilon$ , as  $\alpha$  increase the velocity profile increases while the temperature profile decreases. This may due to the rise in the aligned angle makes magnetic field stronger. When  $\alpha = 0^\circ$  it indicates that there is no magnetic field, but when the  $\alpha = 90^\circ$  the aligned magnetic field behaves like a transverse magnetic field hence it attracts the nanoparticles because of changes in the aligned angle's position. The velocity profiles for both CNTs past a wedge with condition of  $\varepsilon = 0.2$  is the highest followed by  $\varepsilon = 0$  and  $\varepsilon = -0.2$ , while MWCNTs is higher compared to SWCNTs. Meanwhile, the wedge with condition of  $\varepsilon = -0.2$  has the highest temperature followed by the  $\varepsilon = 0$  and  $\varepsilon = 0.2$ .

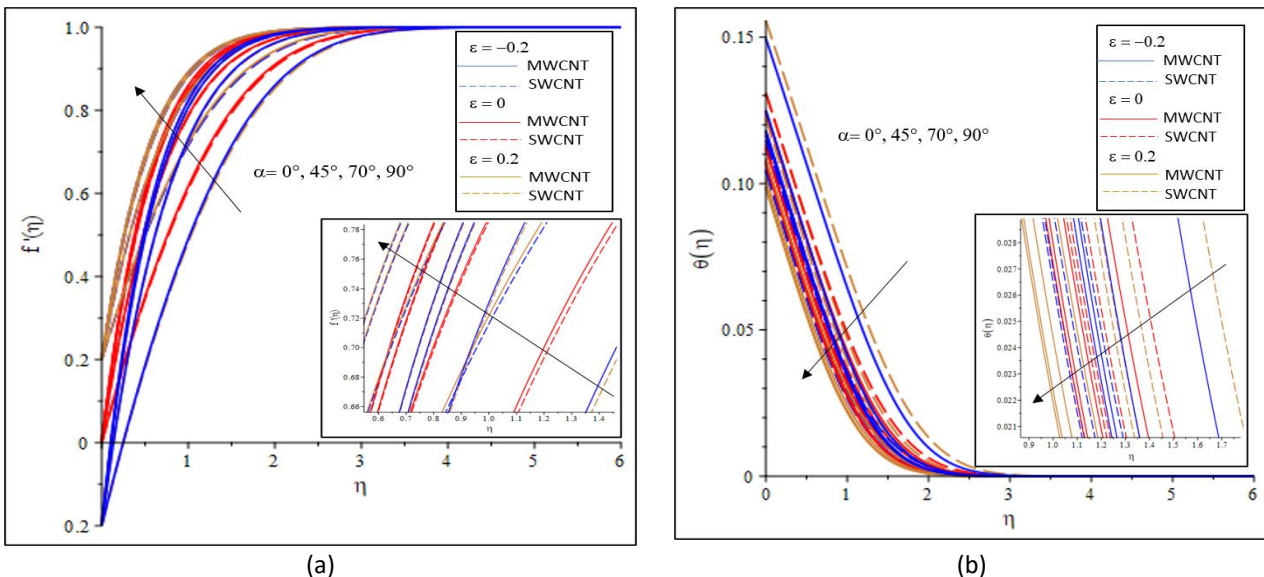


**Fig. 2.** Effects of  $\alpha$  on (a) velocity profiles and (b) temperature profiles

Figure 3(a) and Figure 3(b) illustrates the impact of interaction of magnetic field,  $M$  on velocity and temperature profiles for both SWCNTs and MWCNTs. Meanwhile the other parameters which are  $\lambda = 0.3333$ ,  $\alpha = 45^\circ$ ,  $\lambda_T = 0.3$ ,  $\phi = 0.1$  and  $Bi = 0.1$  are kept constant at for  $\varepsilon = -0.2$ ,  $\varepsilon = 0$  and  $\varepsilon = 0.2$  condition. The magnetic field parameter is denoted as the variable  $M$  which is the ratio of electromagnetic and viscous forces. It serves as a measure of the applied magnetic field's strength. The figure shows a clear indication that the velocity boundary layer's thickness decreases



when the values of  $M$  are increased. It shows that an increase in  $M$ , the velocity profiles increase while temperature profile is decrease for all CNTs wedges. When  $M = 0$ , this indicates there is no magnetic force and with the increment of magnetic field value, it pushes the fluid to the wedge and the momentum boundary layer decreases. When the strength of the magnetic parameter increases, the Lorentz force that is related to the magnetic field thins out the boundary layer. Furthermore, the viscous action decelerates the fluid. The fluid which is decelerated by the viscous action, received a push from the magnetic field which counteracts the viscous effects. From the figure above, the velocity and temperature profiles for the  $\varepsilon = 0.2$  is the highest followed by  $\varepsilon = 0$  and  $\varepsilon = -0.2$ . Also shown that SWCNTs in moving along the flow has the higher velocity profiles compared to MWCNTs while SWCNTs has the higher temperature compared to MWCNTs.

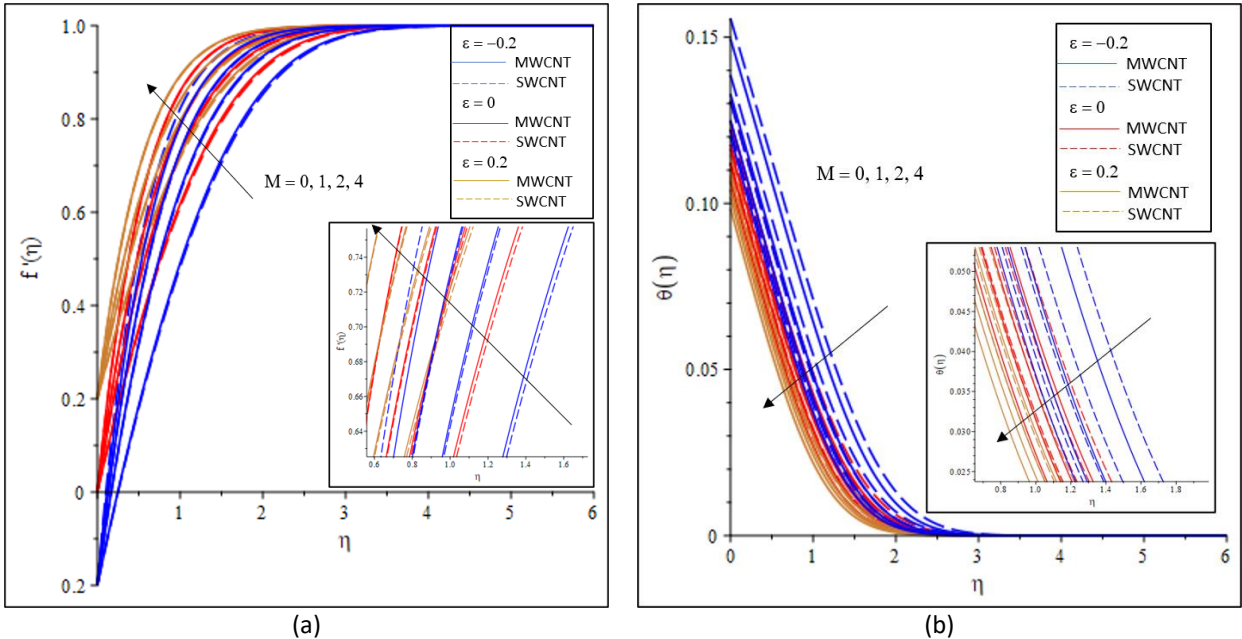
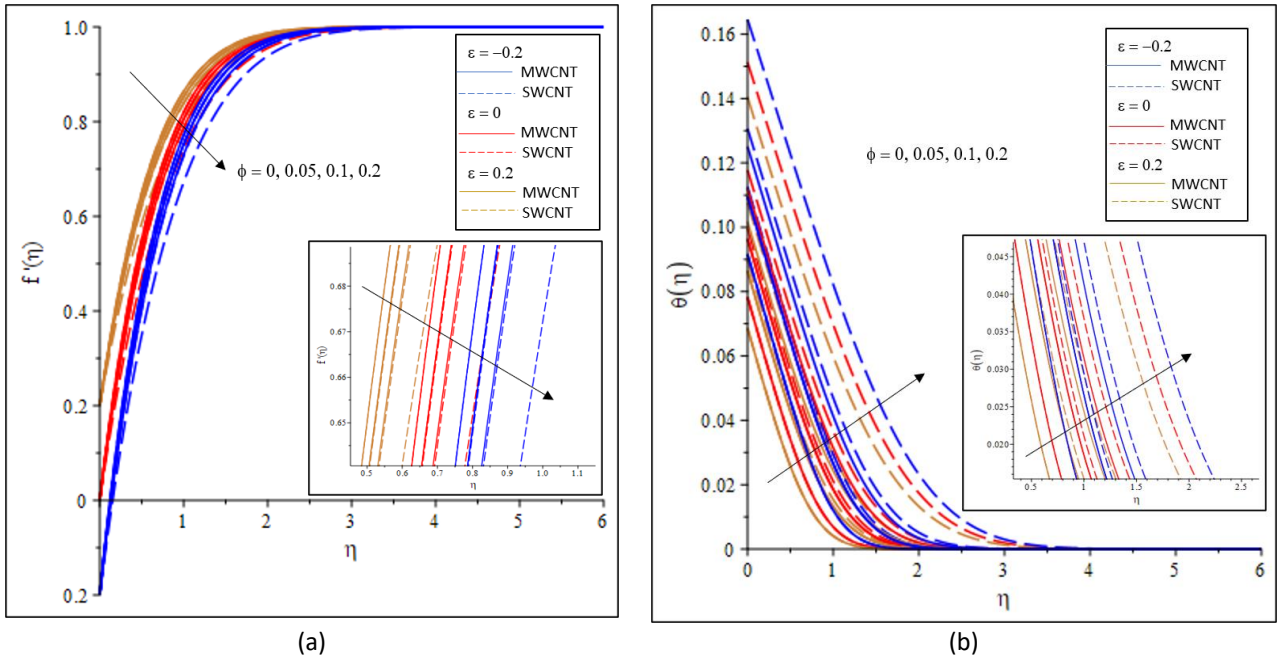


Fig. 3. Effects of  $M$  on (a) velocity profiles and (b) temperature profiles

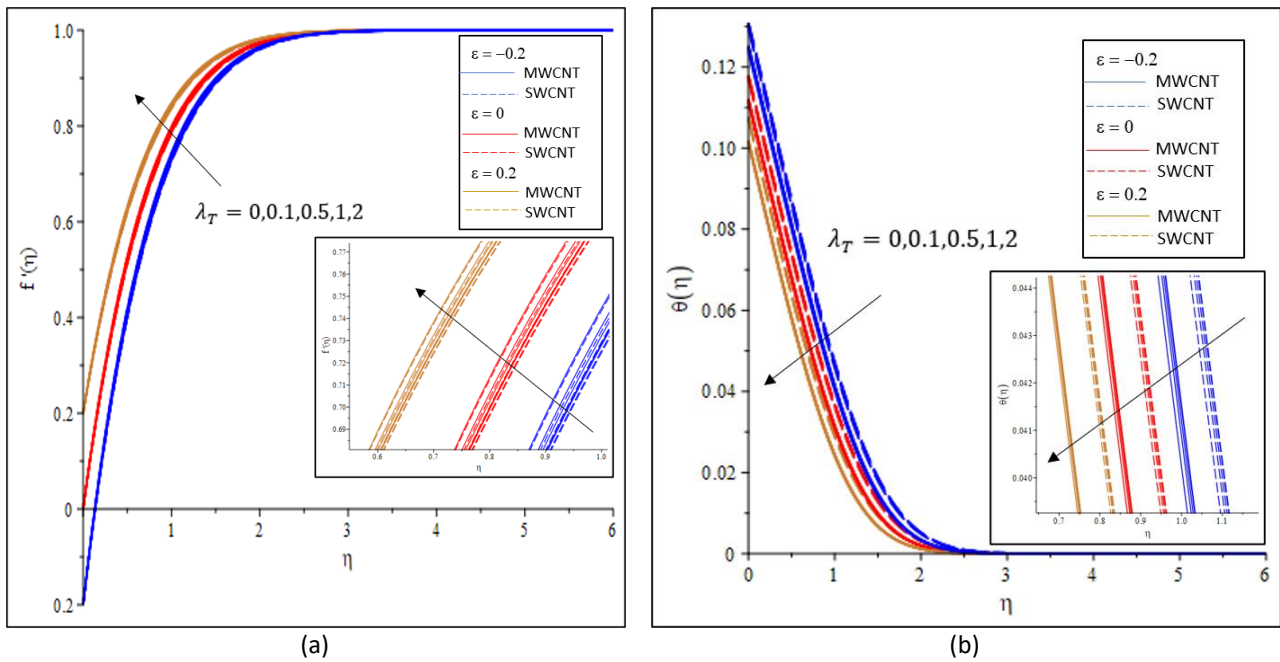
Figure 4(a) and Figure 4(b) shows the of volume fraction of nanoparticles,  $\phi$  on velocity and temperature profiles of SWCNTs and MWCNTs for  $\varepsilon = -0.2, \varepsilon = 0$  and  $\varepsilon = 0.2$ . While the other parameters which are  $\lambda = 0.3333, \alpha = 45^\circ, \lambda_T = 0.3, M = 2$  and  $Bi = 0.1$  are kept constant. It shows that when there is an increase in the  $\phi$ , the velocity profile decreased. Physically, this is due to the reason that an increase in  $\phi$  leads to an increase in the thermal conductivity of the magnetic nanofluid, hence the thickness of the thermal boundary layer increases and viscosity increases and finally velocity decreases. Meanwhile, there is an increase in the magnetic nanofluid temperature, when an increase in  $\phi$ . Furthermore, it tends to go asymptotically to zero as the distance from the boundary increases. An increase in the  $\phi$  increases the nanofluid's thermal conductivity. Another observation when  $\phi$  increases, there is also an increase in the thickness of the thermal boundary layer. The sensitivity thickness of the thermal boundary layer has in terms of  $\phi$  is related to the nanofluid's increased thermal conductivity. This agrees with the physical behaviour that when the  $\phi$  increases, the thermal conductivity, and the thermal boundary layer thickness both increases. Changes in the nanoparticles' shape, size, volume fraction and material allow for tuning so that the heat transfer process can be maximised throughout the fluid volume. This is because the  $\phi$  is dependent on the particle size. Enhancement in thermal conductivity can lead to efficiency improvements, although small, via more effective fluid heat transfer. During the convective heat transfer process in nanofluids, the heat transfer is dependent on the thermal conductivity as well as

other properties like density, the specific heat, and the nanofluid’s dynamic viscosity. Besides that, it is show from the figure above that the  $\varepsilon = 0.2$  has the highest velocity profiles followed by  $\varepsilon = 0$  and  $\varepsilon = -0.2$ . From the graph obtained it shows that MWCNTs of the moving along the flow have the higher velocity profiles compared to SWCNTs while the moving against the flow wedge of SWCNTs has the higher temperature profiles compared with the MWCNTs.



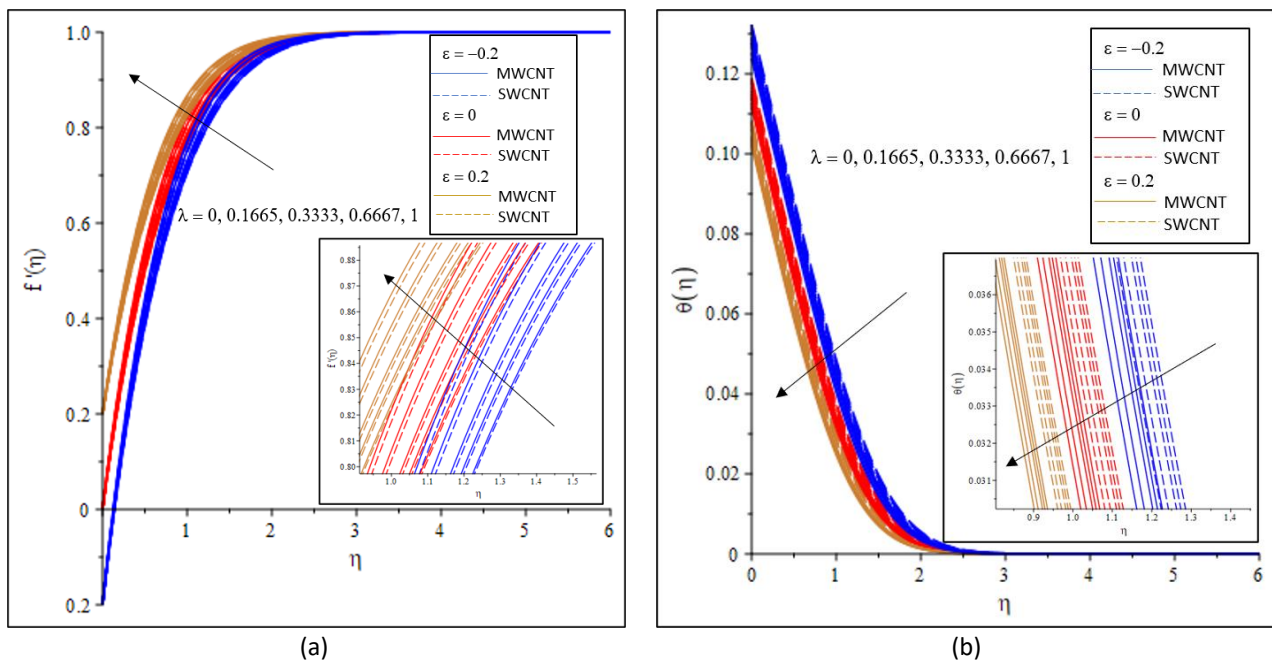
**Fig. 4.** Effects of  $\phi$  on (a) velocity profiles and (b) temperature profiles

Figure 5(a) and Figure 5(b) illustrates the effects of convection parameter,  $\lambda_T$  on velocity and temperature profiles for both SWCNTs and MWCNTs. Meanwhile the other parameters which are  $\alpha = 45^\circ$ ,  $\lambda = 0.3333$ ,  $M = 2$ ,  $\phi = 0.1$  and  $Bi = 0.1$  are kept constant at  $\varepsilon = -0.2$ ,  $\varepsilon = 0$  and  $\varepsilon = 0.2$  condition. It shows when the value  $\lambda_T$  is increase the fluid velocity increases. This happed due to the ratio of buoyancy to viscous forces within the boundary layer. Thus, the fluid viscosity drops with a rise in its values, thus raising the flow velocity. Meanwhile, the thermal buoyancy parameter impacts the non-dimensional temperature in the boundary layer. It shows that temperature in the boundary layer drop monotonically regardless of the convection mode. Furthermore, the thermal boundary layer’s thickness reduces with the rise in the value of  $\lambda_T$ . This is because as  $\lambda_T$  rises, the fluid’s thermal state rises as well, thereby decreasing the rate of heat transfer from the wedge surface to the fluid. Based on the figure shown, the  $\varepsilon = 0.2$  has the highest velocity and temperature profiles followed by  $\varepsilon = 0$  and  $\varepsilon = -0.2$ . Physically, this is because of the larger values of buoyancy force. Also, it shows that MWCNTs of the moving along the flow wedge have the higher velocity profiles compared to SWCNTs while SWCNTs has the higher temperature profiles compared with the MWCNTs.



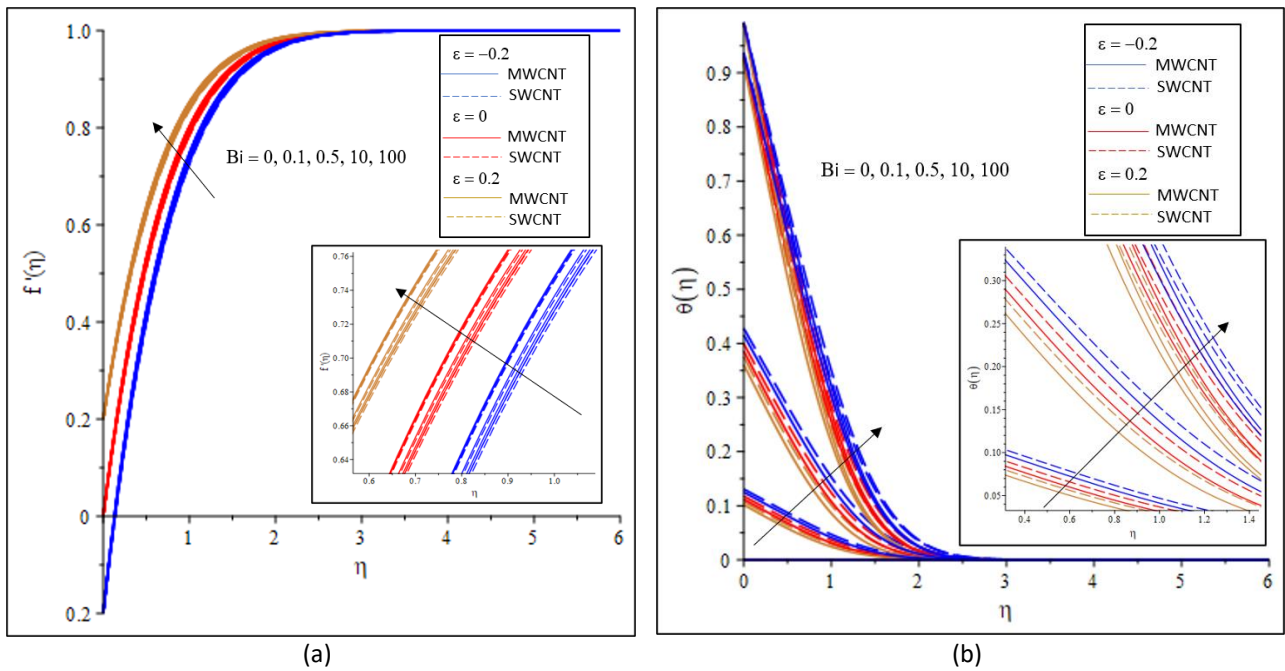
**Fig. 5.** Effects of  $\lambda_T$  on (a) velocity profiles and (b) temperature profiles

Figure 6(a) and Figure 6(b) shows the effect of wedge angle parameter,  $\lambda$  on velocity and temperature profiles of SWCNTs and MWCNTs for  $\varepsilon = -0.2$ ,  $\varepsilon = 0$  and  $\varepsilon = 0.2$ . While the other parameters which are  $\alpha = 45^\circ$ ,  $M = 2$ ,  $\lambda_T = 0.3$ ,  $\phi = 0.1$  and  $Bi = 0.1$  are kept constant. It should be noted that  $\lambda = 0$  represents a vertical wedge angle of  $0^\circ$ ,  $\lambda = 0.1665$  ( $30^\circ$ ) represents the zero degree's wedge angle or a flat wedge,  $\lambda = 0.3333$  represents a vertical wedge or the wedge angle of  $60^\circ$ ,  $\lambda = 0.6667$  represents a vertical wedge or the wedge angle of  $120^\circ$  and  $\lambda = 1$  represents a stagnation point flow or the wedge angle of  $180^\circ$ . From the figure above, it shows an increase of the value of  $\lambda$  for both type of CNTs, the velocity profiles increase while the hydrodynamic boundary layer's thickness decreases. These results coincide with the work of [12,42] that examined how rarefied fluids flow over a wedge. The  $\lambda$  measures the pressure gradient and therefore a positive  $\lambda$  value is an indication of a favourable or negative pressure gradient. Furthermore, if  $\lambda$  is negative, the flow could be considered as decelerating. In this current study, only the positive  $\lambda$  value is considered as a representation of accelerated flows. Thus, for accelerated flows, i.e., positive values of  $\lambda$  velocity profiles squeeze closer and closer to the surface of the wall and hence overshoot or backflow phenomena is difficult to be noticed. Meanwhile, Figure 6(b) shows that there is a decrease in temperature when  $\lambda$  increases. It was also observed that the magnetic nanofluid's maximum temperature was gathered when the flow passes over a flat plate while the minimum value was observed during a stagnation flow. This can be explained by the fact that for  $\lambda = 0$ , the fluid motion's driving force (i.e., the pressure gradient) becomes zero. Thus, at the surface of the wedge, the temperature of the fluid rises. Alternatively, for a rising non-zero  $\lambda$  values, the fluid motion's driving force intensifies. This leads to an accelerated fluid flow and it is also capable of carrying more heat from the wedge's surface to the fluid. Thus, the fluid's temperature at the wedge's surface lowers. The velocity profiles of the  $\varepsilon = 0.2$  is highest followed by  $\varepsilon = 0$  and  $\varepsilon = -0.2$  while the moving along the wedge of MWCNTs has the higher velocity profiles compared to the follow wedge of SWCNTs. Then, for the temperature it can be seen the condition of wedge of the  $\varepsilon = -0.2$  has the highest temperature followed by  $\varepsilon = 0$  and  $\varepsilon = 0.2$  while moving against the flow wedge of SWCNTs shows the higher value than the MWCNTs.



**Fig. 6.** Effects of  $\lambda$  on (a) velocity profiles and (b) temperature profiles

The result on the effect of Biot number,  $Bi$  on velocity and temperature profiles for both SWCNTs and MWCNTs are shown in Figure 7(a) and Figure 7(b). Meanwhile the other parameters which are  $\alpha = 45^\circ$ ,  $M = 2$ ,  $\lambda_T = 0.3$ ,  $\phi = 0.1$  and  $\lambda = 0.3333$  are kept constant at  $\varepsilon = -0.2$ ,  $\varepsilon = 0$  and  $\varepsilon = 0.2$  condition.  $Bi$  is related to the convection heating at the surface it also is an analysis of the relationship of the solid conduction and its surface convection. It shows that when the  $Bi$  increases, the velocity profiles also increase for all types of CNTs. When  $Bi = 0$ , there is no convective heat transfer and the velocity would also be low whereas when  $Bi$  increases, the buoyancy force becomes stronger as a result of the increase in strength of convective process on the wedge. When  $Bi \rightarrow \infty$  convective boundary condition problem reduces to constant wall temperature. It is worth noting that as  $Bi$  rises, so does the temperature profile.  $Bi$  stands for the ratio of the hot fluid edge's convection resistance to the cold fluid edge's convection resistance over the surface. Furthermore, because hot fluid thermal resistance is proportional to  $h_f$ , increasing values of  $Bi$  coincides with a decrease in fluid edge convection. As a result, the thermal boundary layer's width increases. Based on the figure, it shows that the wedge with  $\varepsilon = 0.2$  condition has the highest velocity profiles followed by  $\varepsilon = 0$  and  $\varepsilon = -0.2$  while the wedge with the  $\varepsilon = -0.2$  has the highest temperature profiles than other wedges. Compared between two CNTs that are used, MWCNTs have the higher velocity profiles compared to SWCNTs. Meanwhile, the moving against the flow wedge of SWCNTs is higher temperature compared to MWCNTs.



**Fig. 7.** Effects of  $Bi$  on (a) velocity profiles and (b) temperature profiles

Table 3 presents the variation occurring in skin friction coefficient and Nusselt number for different  $\alpha, M, \lambda, \lambda_T, \phi$  and  $Bi$  values applicable to various wedge movements for SWCNTs-water. For all three cases, it could be clearly seen that all parameters had a boosting effect on the friction factor coefficients and Nusselt number, especially for the case when  $\epsilon = -0.2$  and  $\epsilon = 0.2$  respectively. The highest value could be seen for the case when  $\alpha$ , and  $M$  are modified. It is interesting to note that in the case  $\epsilon = 0.2$ , the friction factor coefficient was found to be lesser than with the cases of  $\epsilon = -0.2$  and  $\epsilon = 0$ . Meanwhile, for Nusselt number the case of  $\epsilon = -0.2$  was found to be lesser than with the cases of  $\epsilon = 0.2$  and  $\epsilon = 0$ .

Table 4 lists the different variations in the skin friction coefficient and Nusselt number for different values of dimensionless parameters for MWCNTs-water. For all three cases, an enhancement was seen in the heat transfer rates with improving values of  $\alpha, M, \lambda, \lambda_T, \phi$  and  $Bi$ , especially for  $\epsilon = 0.2$  can be benefit to the heat transfer rates while for skin friction can be seen in the case of  $\epsilon = -0.2$ . The highest value could be seen for the case when  $\alpha$  and  $\phi$  in the case  $\epsilon = -0.2$  and  $\epsilon = 0.2$  for skin friction and Nusselt number respectively.

Therefore, skin friction for SWCNTs-water has highest value compared to MWCNTs-water while the highest value for Nusselt number is MWCNTs-water compared to SWCNTs-water.

**Table 3**

Variation in Skin Friction Coefficient and Nusselt Number at Different Dimensionless Parameters for SWCNTs Water

$\alpha$	$M$	$\phi$	$Bi$	$\lambda_T$	$\lambda$	SWCNTs-water					
						Skin Friction			Nusselt Number		
						$\varepsilon = -0.2$	$\varepsilon = 0$	$\varepsilon = 0.2$	$\varepsilon = -0.2$	$\varepsilon = 0$	$\varepsilon = 0.2$
0°	2	0.1	0.1	0.3	0.3333	1.333088	1.230641	1.072348	0.300730	0.309530	0.315319
45°						2.536001	2.175688	1.789830	0.309647	0.314242	0.317880
70°						3.164233	2.686635	2.189060	0.312159	0.315828	0.318862
90°						3.332705	2.824478	2.297368	0.312708	0.316188	0.319092
45°	0	0.1	0.1	0.3	0.3333	1.333088	1.230643	1.072348	0.300729	0.309582	0.315319
	1					2.024546	1.765620	1.473505	0.306798	0.312628	0.316909
	2					2.536001	2.175689	1.789830	0.309647	0.314295	0.317879
	4					3.332705	2.824479	2.297368	0.312707	0.316241	0.319092
45°	2	0	0.1	0.3	0.3333	2.177062	1.861353	1.526378	0.111256	0.112894	0.114068
		0.05				2.346209	2.009516	1.650580	0.206966	0.209984	0.212295
		0.1				2.536002	2.175689	1.789832	0.309699	0.314295	0.317933
		0.2				2.995825	2.578129	2.126919	0.541660	0.550269	0.557320
45°	2	0.1	0	0.3	0.3333	2.518886	2.161186	1.777323	0	0	0
			0.1			2.536001	2.175689	1.789830	0.309647	0.314295	0.317879
			0.5			2.574775	2.210268	1.820903	1.018951	1.069752	1.112387
			10			2.640786	2.274974	1.884092	2.251146	2.506239	2.749136
			100			2.647989	2.282609	1.892013	2.387477	2.677701	2.956297
45°	2	0.1	0.1	0	0.3333	2.518886	2.161186	1.777323	0.309557	0.314239	0.317843
				0.1		2.524603	2.166028	1.781496	0.309587	0.314258	0.317855
				0.5		2.547352	2.185322	1.798146	0.309706	0.314332	0.317904
				1		2.575529	2.209282	1.818857	0.309852	0.314424	0.317964
				2		2.631055	2.256691	1.859952	0.310135	0.314604	0.318083
45°	2	0.1	0.1	0.3	0	2.466127	2.095242	1.708869	0.309066	0.313877	0.317590
				0.1665		2.501272	2.135811	1.749785	0.309364	0.314092	0.317739
				0.3333		2.536001	2.175690	1.789830	0.309647	0.314295	0.317879
				0.6667		2.604048	2.253265	1.867277	0.310169	0.314670	0.318139
				1		2.670359	2.328211	1.941584	0.3106423	0.315009	0.318373



**Table 4**  
 Variation of Skin Friction Coefficient and Nusselt Number at Different Dimensionless Parameters for MWCNTs Water

$\alpha$	$M$	$\phi$	$Bi$	$\lambda_T$	$\lambda$	MWCNTs-Water					
						Skin Friction			Nusselt Number		
						$\varepsilon = -0.2$	$\varepsilon = 0$	$\varepsilon = 0.2$	$\varepsilon = -0.2$	$\varepsilon = 0$	$\varepsilon = 0.2$
0°	2	0.1	0.1	0.3	0.3333	1.353150	1.249410	1.088768	0.270116	0.278038	0.283162
45°						2.546419	2.186096	1.799424	0.277899	0.282062	0.285313
70°						3.172519	2.694977	2.196806	0.280109	0.283433	0.286150
90°						3.340558	2.832395	2.304728	0.280591	0.283746	0.286347
45°	0	0.1	0.1	0.3	0.3333	1.353150	1.249410	1.088768	0.270116	0.278038	0.283162
	1					2.037688	1.778573	1.485302	0.275400	0.280629	0.284492
	2					2.546419	2.186096	1.799424	0.277899	0.282062	0.285313
	4					2.969969	2.832395	2.304728	0.279472	0.283746	0.286347
45°	2	0	0.1	0.3	0.3333	2.177062	1.861353	1.526378	0.111256	0.112894	0.114068
		0.05				2.351051	2.014365	1.655061	0.191420	0.194231	0.196362
		0.1				2.546419	2.186096	1.799424	0.277899	0.282062	0.285313
		0.2				3.612818	3.095439	2.543303	0.499799	0.507139	0.512703
45°	2	0.1	0	0.3	0.3333	2.530356	2.172638	1.787921	0	0	0
			0.1			2.546419	2.186096	1.799424	0.277899	0.282062	0.285313
			0.5			2.583602	2.218926	1.828675	0.928061	0.975397	1.014928
			10			2.649442	2.283281	1.891266	2.102674	2.356036	2.595736
			100			2.656921	2.291138	1.899421	2.237973	2.526557	2.803679
45°	2	0.1	0.1	0	0.3333	2.530356	2.172638	1.787921	0.277826	0.282018	0.285285
				0.1		2.535721	2.177130	1.791760	0.277851	0.282033	0.285294
				0.5		2.557075	2.195037	1.807074	0.277947	0.282091	0.285332
				1		2.583536	2.217284	1.826132	0.278066	0.282164	0.285378
				2		2.635714	2.261335	1.863972	0.278295	0.282305	0.285469
45°	2	0.1	0.1	0.3	0	2.468193	2.098288	1.712313	0.276765	0.281061	0.284430
					0.1665	2.508070	2.143103	1.756841	0.277052	0.281264	0.284568
					0.3333	2.547406	2.187076	1.800343	0.277323	0.281456	0.284698
					0.6667	2.624293	2.272410	1.884272	0.277821	0.281807	0.284937
					1	2.698995	2.354612	1.964574	0.278269	0.282122	0.285152

## 5. Conclusions

This paper study on the effects an aligned MHD mixed convection water functionalized CNTs flow over a static or moving wedge with convective boundary condition. The influences of the aligned angle of magnetic field,  $\alpha$ , interaction of magnetic field,  $M$ , volume fraction of nanoparticles,  $\phi$ , wedge angle parameter,  $\lambda$ , Biot number,  $Bi$ , and convection parameter,  $\lambda_T$  on effect of SWCNTs, MWCNTs and base fluid results obtained: example:

- i. As the value of  $\alpha$ ,  $M$ ,  $\lambda$ , and  $\lambda_T$  increases, the velocity profiles increase whereas the temperature profiles decrease.
- ii. As the value of  $\alpha$ ,  $M$ ,  $\lambda$ ,  $\phi$ ,  $Bi$  and  $\lambda_T$  increases, the skin friction and Nusselt number is increasing.
- iii. An increase in  $\phi$  and  $Bi$ , depicts the decrement in velocity profiles meanwhile the temperature profiles increase. Also, the moving against the flow wedge of MWCNTs is the highest skin friction and moving along the flow wedge of SWCNTs is the highest Nusselt number.

- iv. As the increase value of  $\alpha$ ,  $\phi$ ,  $\lambda$ , and  $\lambda_T$ , the moving along with the flow wedge of MWCNTs is the highest velocity profiles. While, moving against the flow wedge of SWCNTs is the highest temperature profiles.
- v. As value in  $M$  increase, the highest velocity profiles and temperature profiles is on moving along the flow wedge of SWCNTs. Meanwhile, the highest skin friction is on moving against the flow wedge of SWCNTs and for the Nusselt number moving along the flow wedge of SWCNTs is the highest.
- vi. With  $Bi$  increasing shows that moving along the flow wedge of MWCNTs has the highest velocity profiles and moving against the flow wedge of SWCNTs has the highest temperature profiles.
- vii. The moving along the flow wedge of MWCNTs has the highest skin friction and moving along the flow wedge of SWCNTs has the highest temperature profile as a  $\lambda_T$  increases.

### Acknowledgement

The authors extend their appreciation to Universiti Teknologi MARA Shah Alam for funding this work through Geran Penyelidikan UMP-IIUM-UiTM Sustainable Research Collaboration 2020 under grant number 600-RMC/SRC/5/3 (016/2020).

### References

- [1] Choi, S. US, and Jeffrey A. Eastman. *Enhancing thermal conductivity of fluids with nanoparticles*. No. ANL/MSD/CP-84938; CONF-951135-29. Argonne National Lab.(ANL), Argonne, IL (United States), 1995.
- [2] Eastman, Jeffery A., U. S. Choi, Shaoping Li, L. J. Thompson, and Shinpyo Lee. "Enhanced thermal conductivity through the development of nanofluids." *MRS Online Proceedings Library (OPL)* 457 (1996): 3. <https://doi.org/10.1557/PROC-457-3>
- [3] Khan, Ibrahim, Khalid Saeed, and Idrees Khan. "Nanoparticles: Properties, applications and toxicities." *Arabian journal of chemistry* 12, no. 7 (2019): 908-931. <https://doi.org/10.1016/j.arabjc.2017.05.011>
- [4] Halefadi, Salma, Thierry Maré, and Patrice Estellé. "Efficiency of carbon nanotubes water based nanofluids as coolants." *Experimental Thermal and Fluid Science* 53 (2014): 104-110. <https://doi.org/10.1016/j.expthermflusci.2013.11.010>
- [5] Baughman, Ray H., Anvar A. Zakhidov, and Walt A. De Heer. "Carbon nanotubes-the route toward applications." *science* 297, no. 5582 (2002): 787-792. <https://doi.org/10.1126/science.1060928>
- [6] O'connell, Michael J. "Carbon nanotubes: properties and applications." *CRC press* (2018).
- [7] Maré, Thierry, Salma Halefadi, Ousmane Sow, Patrice Estellé, Steven Duret, and Frederic Bazantay. "Comparison of the thermal performances of two nanofluids at low temperature in a plate heat exchanger." *Experimental Thermal and Fluid Science* 35, no. 8 (2011): 1535-1543. <https://doi.org/10.1016/j.expthermflusci.2011.07.004>
- [8] Akhilesh, M., K. Santarao, and M. V. S. Babu. "Thermal conductivity of CNT-wated nanofluids: a review." *Mechanics and Mechanical Engineering* 22, no. 1 (2018): 207-220. <https://doi.org/10.2478/mme-2018-0019>
- [9] Falkneb, V. M., and Sylvia W. Skan. "LXXXV. Solutions of the boundary-layer equations." *The London, Edinburgh, and Dublin Philosophical Magazine and Journal of Science* 12, no. 80 (1931): 865-896. <https://doi.org/10.1080/14786443109461870>
- [10] DR, Hartree. "Onan equation occurring in Falkner and Skan's approximate treatment of the equations of the boundary layer." In *Math Proc Camb Philos Soc*, vol. 33, no. 2, pp. 223-239. 1937. <https://doi.org/10.1017/S0305004100019575>
- [11] Koh, J. C. Y., and J. P. Hartnett. "Skin friction and heat transfer for incompressible laminar flow over porous wedges with suction and variable wall temperature." *International Journal of Heat and Mass Transfer* 2, no. 3 (1961): 185-198. [https://doi.org/10.1016/0017-9310\(61\)90088-6](https://doi.org/10.1016/0017-9310(61)90088-6)
- [12] Ilias, Mohd Rijal, Noraihan Afiah Rawi, Noor Hidayah Mohd Zaki, and Sharidan Shafie. "Aligned mhd magnetic nanofluid flow past a static wedge." *Int. J. Eng. Technol* 7, no. 3.28 (2018): 28-31. <https://doi.org/10.14419/ijet.v7i3.28.20960>
- [13] Ilias, Mohd Rijal, Ismail N. S'aidah, W. S. Esah, and C. Hussain. "Unsteady aligned MHD boundary layer flow of a magnetic nanofluid over a wedge." *International Journal of Civil Engineering and Technology (IJCET)* 9 (2018): 794-810.



- [14] Ilias, MOHD RIJAL. "Steady and Unsteady Aligned Magnetohydrodynamics Free Convection Flows of Magnetic and Non Magnetic Nanofluids along a Wedge, Vertical and Inclined Plates." *Vertical and Inclined Plates, Universiti Teknologi Malaysia* (2018).
- [15] Pandey, A. K., and M. Kumar. "Chemical reaction and thermal radiation effects on a boundary layer flow of nanofluid over a wedge with viscous and Ohmic dissipation, St. Petersburg Polytechnical State University Journal." *Physics and Mathematics* 10, no. 4 (2017): 54-72. <https://doi.org/10.1016/j.spjpm.2017.10.008>
- [16] Ishak, Siti Shuhada, Nurul Nurfatihah Mazlan, Mohd Rijal Ilias, Roselah Osman, Abdul Rahman Mohd Kasim, and Nurul Farahain Mohammad. "Radiation Effects on Inclined Magnetohydrodynamics Mixed Convection Boundary Layer Flow of Hybrid Nanofluids over a Moving and Static Wedge." *Journal of Advanced Research in Applied Sciences and Engineering Technology* 28, no. 3 (2022): 68-84. <https://doi.org/10.37934/araset.28.3.6884>
- [17] Kandasamy, R., I. Muhaimin, and Radiah Mohammad. "Single walled carbon nanotubes on MHD unsteady flow over a porous wedge with thermal radiation with variable stream conditions." *Alexandria Engineering Journal* 55, no. 1 (2016): 275-285. <https://doi.org/10.1016/j.aej.2015.10.006>
- [18] Berrehal, Hamza, and Abdelaziz Maougal. "Entropy generation analysis for multi-walled carbon nanotube (MWCNT) suspended nanofluid flow over wedge with thermal radiation and convective boundary condition." *Journal of Mechanical Science and Technology* 33, no. 1 (2019): 459-464. <https://doi.org/10.1007/s12206-018-1245-y>
- [19] Amar, N. "Viscous dissipation and heat transfer effect on MHD boundary layer flow past a wedge of nano fluid embedded in a porous media." *Turkish Journal of Computer and Mathematics Education (TURCOMAT)* 12, no. 4 (2021): 1352-1366. <https://doi.org/10.17762/turcomat.v12i4.1208>
- [20] Venkataramanaiah, G., M. Sreedhar Babu, and M. Lavanya. "Convective heat transfer in Water Functionalized Carbon Nanotube Flow past a Static/Moving wedge with heat source/sink." <https://doi.org/10.18535/ijecs/v5i2.22>
- [21] Khan, Waqar A., Richard Culham, and Rizwan Ul Haq. "Heat transfer analysis of MHD water functionalized carbon nanotube flow over a static/moving wedge." *Journal of Nanomaterials* 16, no. 1 (2015): 112-112. <https://doi.org/10.1155/2015/934367>
- [22] Noranuar, Wan Nura'in Nabilah, Ahmad Qushairi Mohamad, Sharidan Shafie, Ilyas Khan, Mohd Rijal Ilias, and Lim Yeou Jiann. "Analysis of Heat Transfer in Non-Coaxial Rotation of Newtonian Carbon Nanofluid Flow with Magnetohydrodynamics and Porosity Effects." *21st Century Nanostructured Materials* (2021): 93. <https://doi.org/10.5772/intechopen.100623>
- [23] Noranuar, Wan Nura'in Nabilah, Ahmad Qushairi Mohamad, Sharidan Shafie, Ilyas Khan, Lim Yeou Jiann, and Mohd Rijal Ilias. "Non-coaxial rotation flow of MHD Casson nanofluid carbon nanotubes past a moving disk with porosity effect." *Ain Shams Engineering Journal* 12, no. 4 (2021): 4099-4110. <https://doi.org/10.1016/j.asej.2021.03.011>
- [24] Alqahtani, Bader, Zafar Mahmood, Maryam Ahmed Alyami, Abeer M. Alotaibi, Umar Khan, and Ahmed M. Galal. "Heat and mass transfer analysis of MHD stagnation point flow of carbon nanotubes with convective stretching disk and viscous dissipation." *Advances in Mechanical Engineering* 14, no. 10 (2022): 16878132221128390. <https://doi.org/10.1177/16878132221128390>
- [25] Nayan, Asmahani, Nur Izzatie Farhana Ahmad Fauzan, Mohd Rijal Ilias, Shahida Farhan Zakaria, and Noor Hafizah Zainal Aznam. "Aligned Magnetohydrodynamics (MHD) Flow of Hybrid Nanofluid Over a Vertical Plate Through Porous Medium." *Journal of Advanced Research in Fluid Mechanics and Thermal Sciences* 92, no. 1 (2022): 51-64. <https://doi.org/10.37934/arfmts.92.1.5164>
- [26] Ilias, Mohd Rijal, Noraihan Afiqah Rawi, and Sharidan Shafie. "Steady aligned MHD free convection of Ferrofluids flow over an inclined plate." *Journal of Mechanical Engineering (JMEchE)* 14, no. 2 (2017): 1-15.
- [27] Ismail, Nur Suhaida Aznidar, Ahmad Sukri Abd Aziz, Mohd Rijal Ilias, and Siti Khuzaimah Soid. "Mhd boundary layer flow in double stratification medium." In *Journal of Physics: Conference Series* 1770, no. 1, (2021): 012045. <https://doi.org/10.1088/1742-6596/1770/1/012045>
- [28] Watanabe, T. "Thermal boundary layers over a wedge with uniform suction or injection in forced flow." *Acta Mechanica* 83, no. 3 (1990): 119-126. <https://doi.org/10.1007/BF01172973>
- [29] Yih, K. A. "Uniform suction/blowing effect on forced convection about a wedge: uniform heat flux." *Acta Mechanica* 128, no. 3 (1998): 173-181. <https://doi.org/10.1007/BF01251888>
- [30] Mabood, Fazle, Anum Shafiq, Waqar Ahmed Khan, and Irfan Anjum Badruddin. "MHD and nonlinear thermal radiation effects on hybrid nanofluid past a wedge with heat source and entropy generation." *International Journal of Numerical Methods for Heat & Fluid Flow* 32, no. 1 (2022): 120-137. <https://doi.org/10.1108/HFF-10-2020-0636>
- [31] Mishra, P., M. R. Acharya, and S. Panda. "Mixed convection MHD nanofluid flow over a wedge with temperature-dependent heat source." *Pramana* 95, no. 2 (2021): 1-12. <https://doi.org/10.1007/s12043-021-02087-z>
- [32] Waini, Iskandar, Anuar Ishak, Teodor Groşan, and Ioan Pop. "Mixed convection of a hybrid nanofluid flow along a vertical surface embedded in a porous medium." *International Communications in Heat and Mass Transfer* 114 (2020): 104565. <https://doi.org/10.1016/j.icheatmasstransfer.2020.104565>

- [33] Rawi, Noraihan Afiqah, Mohd Rijal Ilias, Zaiton Mat Isa, and Sharidan Shafie. "G-Jitter induced mixed convection flow and heat transfer of micropolar nanofluids flow over an inclined stretching sheet." In *AIP Conference Proceedings* 1775, no. 1, (2016): 030020. <https://doi.org/10.1063/1.4965140>
- [34] Ismail, M. A., N. F. Mohamad, M. R. Ilias, and S. Shafie. "MHD Effect on Unsteady Mixed Convection Boundary Layer Flow past a Circular Cylinder with Constant Wall Temperature." In *Journal of Physics: Conference Series* 890, no. 1, (2017): 012054. <https://doi.org/10.1088/1742-6596/890/1/012054>
- [35] Anuar, Nur Syazana, Norfifah Bachok, Norihan Md Arifin, and Haliza Rosali. "Analysis of Al<sub>2</sub>O<sub>3</sub>-Cu nanofluid flow behaviour over a permeable moving wedge with convective surface boundary conditions." *Journal of King Saud University-Science* 33, no. 3 (2021): 101370. <https://doi.org/10.1016/j.jksus.2021.101370>
- [36] Hussain, Majid, Abdul Ghaffar, Akhtar Ali, Azeem Shahzad, Kottakkaran Sooppy Nisar, M. R. Alharthi, and Wasim Jamshed. "MHD thermal boundary layer flow of a Casson fluid over a penetrable stretching wedge in the existence of nonlinear radiation and convective boundary condition." *Alexandria Engineering Journal* 60, no. 6 (2021): 5473-5483. <https://doi.org/10.1016/j.aej.2021.03.042>
- [37] Ilias, Mohd Rijal, Noraihan Afiqah Rawi, and Sharidan Shafie. "Natural convection of ferrofluid from a fixed vertical plate with aligned magnetic field and convective boundary condition." *Malaysian Journal of Fundamental and Applied Sciences* 13, no. 3 (2017). <https://doi.org/10.11113/mjfas.v13n3.651>
- [38] Bosli, Fazillah, Alia Syafiqah Suhaimi, Siti Shuhada Ishak, Mohd Rijal Ilias, Amirah Hazwani Abdul Rahim, and Anis Mardiana Ahmad. "Investigation of Nanoparticles Shape Effects on Aligned MHD Casson Nanofluid Flow and Heat Transfer with Convective Boundary Condition." *Journal of Advanced Research in Fluid Mechanics and Thermal Sciences* 91, no. 1 (2022): 155-171. <https://doi.org/10.37934/arfmts.91.1.155171>
- [39] Rosaidi, Nor Alifah, Nurul Hidayah Ab Raji, Siti Nur Hidayatul Ashikin Ibrahim, and Mohd Rijal Ilias. "Aligned magnetohydrodynamics free convection flow of magnetic nanofluid over a moving vertical plate with convective boundary condition." *Journal of Advanced Research in Fluid Mechanics and Thermal Sciences* 93, no. 2 (2022): 37-49. <https://doi.org/10.37934/arfmts.93.2.3749>
- [40] Hone, J. "Carbon nanotubes: thermal properties." *Dekker Encyclopedia of Nanoscience and nanotechnology* 7 (2004): 603-610.
- [41] Ruoff, Rodney S., and Donald C. Lorents. "Mechanical and thermal properties of carbon nanotubes." *carbon* 33, no. 7 (1995): 925-930. [https://doi.org/10.1016/0008-6223\(95\)00021-5](https://doi.org/10.1016/0008-6223(95)00021-5)
- [42] Rahman, M. M., and I. A. Eltayeb. "Convective slip flow of rarefied fluids over a wedge with thermal jump and variable transport properties." *International Journal of Thermal Sciences* 50, no. 4 (2011): 468-479. <https://doi.org/10.1016/j.ijthermalsci.2010.10.020>